[5] K. H. Berkner, S. N. Kaplan, and R. V. Pyle, Phys. Rev. 134, A1461 (1964).
[6] S. K. Allison, Rev. Mod. Phys. 30, 1137 (1958).
[7] I. S. Dmitriev and V. S. Nikolaev, Zh. Eksperim. i Teor. Fiz. 44, 660 (1963) [English transl.: Soviet Phys. – JETP 17, 447 (1963)].
[8] N. F. Mott and H. S. W. Massey, The Theory of Atomic Collisions (Oxford University Press, New York, 1965), 3rd Ed.
[9] Y. K. Kim and M. Inokuti, Phys. Rev. 165, 39 (1968).
[10] J. F. Hart and G. Herzberg, Phys. Rev. 106, 79 (1957).
[11] International Tables of X-Ray Crystallography, (The Kynoch Press, Birmingham, England, 1962), Vol. III.
[12] D. T. Cromer and J. B. Mann, J. Chem. Phys. 47, 1892 (1967).

PHYSICAL REVIEW VOLUME 184, NUMBER 1 5 AUGUST 1969

Differential Elastic and Rotational Excitation Cross Sections for Electron-H_2 Scattering*

Neal F. Lane†
Department of Physics, Rice University, Houston, Texas 77001
and
S. Geltman‡
Joint Institute for Laboratory Astrophysics, University of Colorado, Boulder, Colorado 80302

(Received 24 February 1969)

Differential elastic and rotational excitation cross sections for electron-H_2 scattering have been calculated in the close-coupling approximation with electron exchange neglected. The resulting elastic angular distributions are found to be in very good agreement with measurements. An apparent oscillation in the measured differential cross section for rotational excitation is not found in the calculation.

I. INTRODUCTION

In a previous paper on rotational excitation of H_2 by slow electron impact[1] (will be referred to as LGI), we described in detail the close-coupling method (without exchange) applied to electron-molecule scattering and presented calculated elastic and rotational-excitation cross sections for a variety of different rotational states and energies. It was pointed out that rotational excitation is dominated by p-wave scattering. Differential cross sections were not calculated at that time, since measurements of angular distributions of rotational-excitation cross sections for molecules seemed rather far in the future. Only a year later, however, Ehrhardt and Linder reported[2] their differential measurements of elastic and rotational-excitation cross sections for electrons in H_2. These authors noted that the integrated $j = 1 \rightarrow 3$ excitation cross section was in good agreement with our calculations. The angular distribution, however, did not show a pronounced minimum at 90° and therefore, the authors argued, could not arise principally from p-wave scattering. Thus, it seemed worthwhile to calculate the differential cross sections and make direct comparisons.

II. THEORY

The details of the close-coupling formalism as well as a full discussion of the numerical methods, choice of electron-molecule potentials, treatment of polarization, and other relevant material are all given in LGI[1] and will not be repeated here. One can summarize the close-coupling calculation as follows: (i) The total scattering wave function is expanded in terms of the set of eigenfunctions of J^2 and J_z, where $\vec{J}=j$ (molecular rotation) $+\,l$ (electron partial-wave orbital angular momentum). (ii) The coefficients in such an expansion satisfy a set of coupled differential equations in r, the radial coordinate of the scattered electron, and their asymptotic behavior defines the scattering matrix for the electron-molecule collision problem. Once the S matrix is determined, the differential cross sections may be obtained from the expression[3] (all cross sections are in $a_0{}^2$)

$$\frac{d\sigma(j'\leftarrow j)}{d\Omega}=\left(\frac{(-1)^{j'-j}m}{4(2j+1)k_j{}^2}\right)\cdot\sum_{\lambda=0}^{\infty}A_\lambda(j'\leftarrow j)\times P_\lambda(\cos\theta)\,,\qquad(1)$$

where $k_j{}^2$ is the incident electron energy in Ry, and where

$$A_\lambda(j'\leftarrow j)=\sum_{J_1}\sum_{J_2}\sum_{l_1}\sum_{l_2}\sum_{l_1'}\sum_{l_2'}\times Z(l_1J_1l_2J_2;j\lambda)Z(l_1'J_1l_2'J_2;j'\lambda)\times T^{J_1}(j'l_1';jl_1)^*\,T^{J_2}(j'l_2';jl_2)\,,\qquad(2)$$

and
$$Z(abcd;ef)=(-1)^{\frac{1}{2}(f-a+c)}\times[(2a+1)(2b+1)(2c+1)(2d+1)]^{\frac{1}{2}}\times(acoo\,|\,acfo)\,W(abcd;ef),\qquad(3)$$

the last two factors being Clebsch-Gordan and Racah coefficients, respectively.

In Eq. (2), the last two factors are T-matrix elements, defined in terms of the S matrix by[1]

$$T^J(j'l',jl)=\delta_{jj'}\delta_{ll'}-S^J(j'l',jl),\qquad(4)$$

where the indices J, j, and l refer, respectively, to the total, molecular-rotation, and partial-wave angular momenta, and taken together define a single channel of the scattering. In the summation over l_1, l_2, l_1', and l_2', the limits of summation are determined by the relations

$$|J_1-j|\leq l_1\leq J_1+j,$$

and
$$|J_2-j|\leq l_2\leq J_2+j,\qquad(5)$$

and similar relations for l_1' and l_2', involving j'. As a practical matter, the sums in Eqs. (1) and (2) are essentially finite, since we have found it necessary to consider only a few j levels at a time. At low energies, the T-matrix elements corresponding to large values of l or l' are very small,[1] hence only a few values of J need be considered. The Clebsch-Gordan coefficient in Eq. (3) then constrains λ in Eq. (1) to be no greater than l_1+l_2 or $l_1'+l_2'$, whichever is smaller.

We shall also have reason to refer to the integrated cross sections[3] for elastic scattering ($j'=j$) and rotational excitation ($j'\neq j$)

$$\sigma(j'\leftarrow j)=\frac{\pi(-1)^{j'-j}}{(2j+1)k_j{}^2}A_0(j'\leftarrow j)$$
$$=\frac{\pi}{(2j+1)k_j{}^2}\sum_J\sum_l\sum_{l'}(2J+1)\times|T^J(j'l';jl)|^2,\qquad(6)$$

and momentum transfer in elastic scattering

$$\sigma_m(j\leftarrow j)=\int(1-\cos\theta)\,d\sigma(j\leftarrow j)$$
$$=\frac{\pi}{(2j+1)k_j{}^2}\left[A_0(j\leftarrow j)-\tfrac{1}{3}A_1(j\leftarrow j)\right].\qquad(7)$$

III. ELECTRON-H_2 INTERACTION POTENTIAL

In LGI, the electron-H_2 interaction was taken as

$$V(\vec{r},\hat{s})=\sum_{\mu=0}^{4}v_\mu{}^B(r)P_\mu(\hat{r}\cdot\hat{s})\,,\qquad(8)$$

where $\vec{r}$ and $\hat{s}$ are the radius vector of the scattered electron and the orientation of the internuclear axis, respectively. The radial potential functions are given as

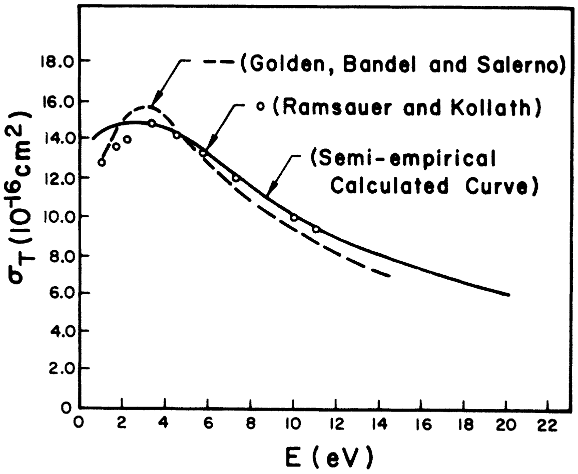

FIG. 1. Total scattering cross sections: Semiempirical calculations (Ref. 1) (solid line); measurements of Golden, Bandel, and Salerno (Ref. 5) (dashed curve); and Ramsauer and Kollath (Ref. 6) (open circles).

$$v_{\mu}^{B}(r) = v_{\mu}^{W}(r)B(r) + v_{\mathrm{LR}\mu}(r), \tag{9}$$

where the $v_{\mu}^{W}(r)$ are short-range interaction terms appropriate to the Wang ground-state wave function.[1,4] The long-range interaction is described by the terms

$$\begin{aligned} v_{\mathrm{LR0}}(r) &= -(\alpha/2r^4)C(r)\,, \\ v_{\mathrm{LR2}}(r) &= -(\alpha'/2r^4 + Q/r^3)C(r)\,, \\ v_{\mathrm{LR4}}(r) &= 0\,, \end{aligned} \tag{10}$$

where the cutoff factor is defined as

$$C(r) = 1 - \exp[-(r/R)^6]\,, \tag{11}$$

R being a free parameter which controls the long-range interaction and must be chosen carefully. In Eq. (9), the short-range interaction terms are shown multiplied by a term $B(r)$, defined by

$$\begin{aligned} B(r) &= \exp[-B(\tfrac{1}{2}s - r)], \quad & r \leq \tfrac{1}{2}s \\ &= 1, & r > \tfrac{1}{2}s\,, \end{aligned} \tag{12}$$

where s is the internuclear separation, $1.4a_0$ for H_2, and B is a parameter which modifies the short-range interaction. In LGI, the point was made in relation to the two parameters, that the rotational-excitation cross section, which is dominated by p-wave scattering, is dependent on R but quite insensitive to variations in B. The parameter R was then chosen by requiring that the calculated[1] and measured[5] total cross sections be in reasonable agreement for energies above about 5 eV, where the p-wave contribution to the total cross section is substantial. A suitable choice was found to be $R = 1.8a_0$. The short-range parameter B is essentially found to modify s-wave scattering only. In a crude way, then, B corrects for the omission of electron exchange, which is very important in s-wave scattering, particularly for energies below 5 eV. An appropriate value was found to be $B = -2.5$. In Fig. 1, the calculated total cross sections, elastic plus rotational excitation, resulting from these choices of the parameters are compared with the measurements of Ramsauer and Kollath[6] and Golden, Bandel, and Salerno.[5] We have found the total cross section to be quite independent of the rotational angular momentum j of the target H_2, so that the calculated curve in Fig. 1 is the same for $j = 0$, 1, etc. This was verified in LGI by direct calculation for values up through $j = 3$.

IV. RESULTS

In Fig. 2, the calculated $j = 1 \rightarrow 3$ rotational-excitation cross sections, integrated over all angles, are compared with the measurements of Ehrhardt and Linder.[2] Considering the approximations made in deriving an appropriate electron-molecule interaction potential and the neglect of exchange in the analysis of the scattering, the agreement is considered to be very good. The agreement is better at lower energies, the calculations apparently being good to better than 3% for energies less than 0.1 eV.[7] It should also be pointed out that the maxima in the calculated and observed cross-section curves both occur at about the same energy, viz., $E \approx 4.5$–5.5 eV. One finds, upon examining the partial-wave contributions to the elastic cross section, that the p-wave elastic partial cross section also has a maximum at about this energy.

The calculated differential elastic and rotational-excitation cross sections for energies between 1 and 10 eV are compared with the measurements of Ehrhardt and Linder[2] and Ramsauer and Kollath[6] in Figs. 3–7. Rather than normalizing Ehrhardt and Linder's data to the total cross section measurements of Golden, Bandel, and Salerno,[5] we chose to simply compare the shapes of the differential elastic cross sections. Thus, in all cases, the elastic cross-section data of Ehrhardt and Linder were scaled so as to agree with the calculated cross section at 90°. A comparison of

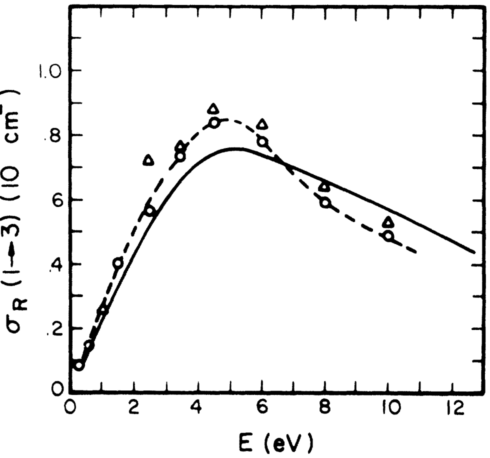

FIG. 2. Rotational-excitation cross sections for the $j = 1 \rightarrow 3$ transition: semiempirical calculations (Ref. 1) (solid line); original measurements of Ehrhardt and Linder (Ref. 2) (open triangles); recent measurements of Ehrhardt and Linder (private communication) (open circles and dashed curve fit).

the calculated and observed integrated cross sections has already been given in Fig. 1. The elastic data of Ramsauer and Kollath[6] are absolute and have not been scaled. The observed and calculated elastic angular distributions are seen to agree well for all energies considered.

In order to compare the calculated and observed rotational-excitation differential cross sections, we have simply scaled the experimental data so that the arithmetic mean of the measured cross sections agrees with that of the calculated cross sections over the angular range covered in the experiment. It should be remarked again here that the dominant contribution to these cross sections is p-wave scattering $(l = l' = 1)$.[1] The angular distributions do not, however, show marked minima at 90°. This is because in the electron-molecule problem, the interaction potential is highly nonspherical and the partial-wave representation is essentially an expansion in spherical harmonics $Y_{lm}(\theta, \varphi)$ instead of the simple Legendre polynomials.[3] Thus, p-wave scattering in the present context includes scattering amplitudes for $m = 0$ and $m = \pm 1$, which have θ dependence $\cos\theta$ and $\sin\theta$, respectively. The differential cross section, containing a mixture of these, does not show a deep minimum at 90°. Also, it should be noted that, while p-wave scattering is dominant, details in the angular variation of the differential rotational-excitation cross section do depend on s, d, and f waves as well, particularly at low energies of the order 1 eV or less.

The much lower signals in the measurement of rotational excitation as compared with elastic scattering cross sections leads to more scatter

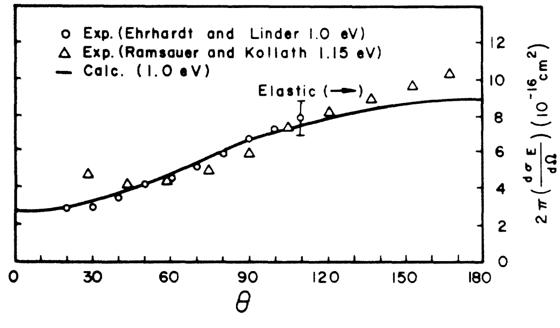

FIG. 3. Differential elastic scattering cross sections $(j = 1)$, present calculations (solid curve) at 1.0 eV; absolute measurements of Ramsauer and Kollath (Ref. 6) at 1.15 eV (open triangles); measurements of Ehrhardt and Linder (Ref. 2) at 1.0 eV scaled to agree with the calculations at 90° (open circles).

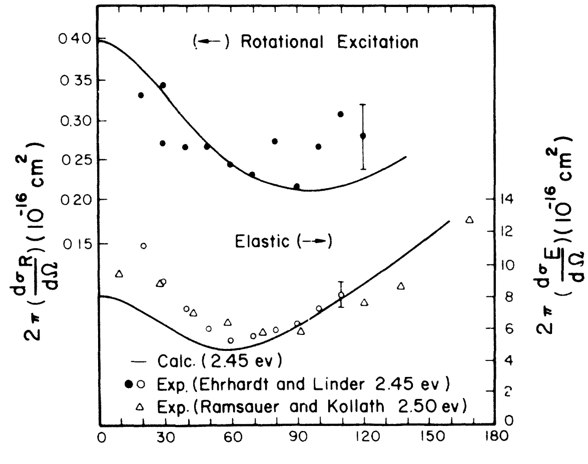

FIG. 4. Differential $j = 1 \rightarrow 3$ rotational-excitation and elastic $(j = 1)$ scattering cross sections: present calculations at 2.45 eV (solid curves); measured rotational-excitation cross sections of Ehrhardt and Linder (Ref. 2) at 2.45 eV (closed circles); absolute elastic cross-section measurements of Ramsauer and Kollath (Ref. 6) at 2.5 eV (open triangles); elastic cross-section measurements of Ehrhardt and Linder (Ref. 2) at 2.45 eV scaled to agree with the calculations at 90° (open circles).

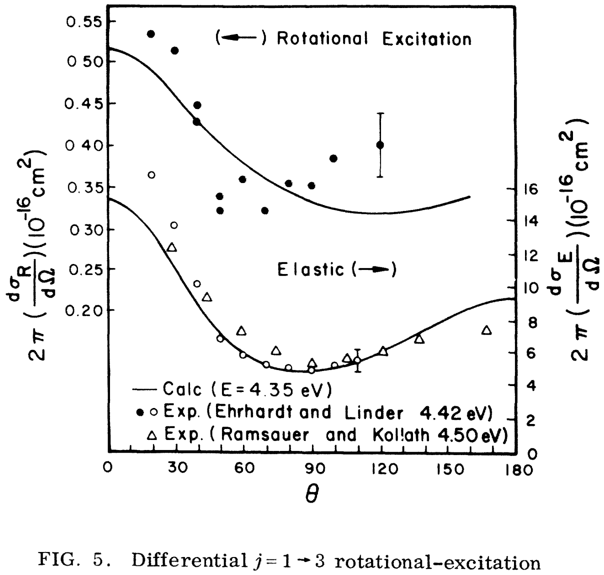

FIG. 5. Differential $j = 1 \rightarrow 3$ rotational-excitation and elastic $(j = 1)$ scattering cross sections; present calculation at 4.35 eV (solid curves); measured rotational-excitation cross section of Ehrhardt and Linder (Ref. 2) at 4.42 eV (closed circles); absolute elastic cross-section measurements of Ramsauer and Kollath (Ref. 6) at 4.5 eV (open triangles); elastic cross-section measurements of Ehrhardt and Linder (Ref. 2) at 4.42 eV scaled to agree with the calculations at 90° (open circles).

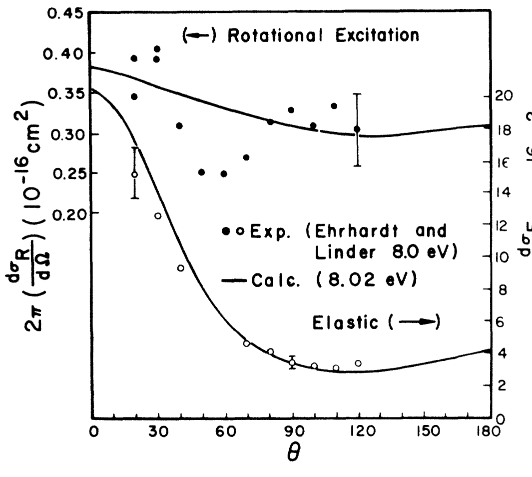

FIG. 6. Differential $j=1\rightarrow3$ rotational-excitation and elastic ($j=1$) scattering cross sections: present calculation at 8.02 eV (solid curves); measured rotational-excitation cross section of Ehrhardt and Linder (Ref. 2) at 8.0 eV (closed circles); elastic cross-section measurements of Ehrhardt and Linder (Ref. 2) at 8.0 eV, scaled to agree with the calculations at 90° (open circles).

of the data points in the former case and a larger error bar assignment. In spite of this, the rotational-excitation data still suggests the presence of large amplitude oscillations in the differential cross sections, which we do not find in the calculated results. A recent, more detailed calculation,[8] which takes full account of exchange effects, results in differential cross sections similar to those reported here. Again, there is no evidence of pronounced oscillations.

We have also calculated elastic-momentum-transfer cross sections. Since momentum transfer emphasizes back scattering, it is apparent from the measured and calculated elastic differential cross sections in Figs. 3–7, that the momentum-transfer cross section should be greater than the elastic cross sections, certainly for energies less than 4.35 eV, the reverse being true at higher energies. Momentum-transfer cross sections calculated according to Eq. (7) are compared in Fig. 8 with the elastic cross section and with the measurements of Engelhardt and Phelps[9] and Bekefi and Brown.[10]

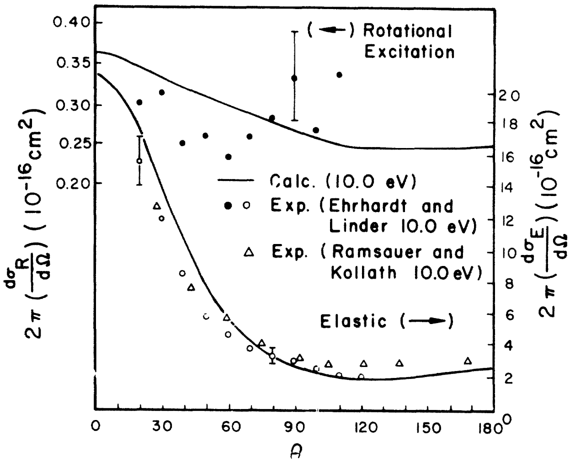

FIG. 7. Differential $j=1\rightarrow3$ rotational-excitation and elastic ($j=1$) scattering cross sections; present calculation at 10.0 eV (solid curves); measured rotational-excitation cross section of Ehrhardt and Linder (Ref. 2) at 10.0 eV (closed circles); absolute elastic cross-section measurements of Ramsauer and Kollath (Ref. 6) at at 10.0 eV (open triangles); elastic cross-section measurements of Ehrhardt and Linder (Ref. 2) at 10.0 eV scaled to agree with the calculations at 90° (open circles).

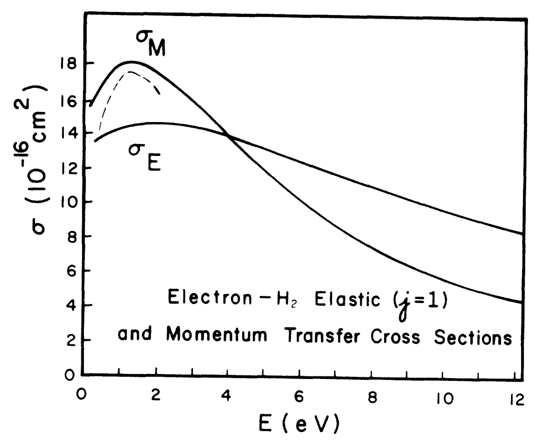

FIG. 8. Comparison of momentum-transfer and total cross sections: calculated momentum-transfer (M) and elastic (E) cross sections for the $j=1$ rotational state (solid curves); momentum-transfer measurements of Engelhardt and Phelps (Ref. 9) and Bekefi and Brown (Ref. 10) (dashed curve). (A comparison of calculated and measured total cross sections is given in Fig. 1.)

---

[*] Research supported by the U. S. Atomic Energy Commission and the Advanced Research Projects Agency of the Department of Defense monitored by Army Research Office, Durham, under contract No. DA-31-124-ARO-D-139.

[†] Alfred P. Sloan Foundation Fellow.

[‡] Laboratory Astrophysics Division, National Bureau of Standards.

[1] N. F. Lane and S. Geltman, Phys. Rev. 160, 53 (1967).

[2] H. Ehrhardt and F. Linder, Phys. Rev. Letters 21, 419 (1968); and private communication.

[3] A. M. Arthurs and A. Dalgarno, Proc. Roy. Soc. (London) A256, 540 (1960).

[4] S. C. Wang, Phys. Rev. 31, 579 (1928).

[5] D. E. Golden, H. W. Bandel, and J. A. Salerno, Phys. Rev. 146, 40 (1966).

[6] C. Ramsauer and R. Kollath, Ann. Physik 4, 91 (1929).

[7] R. W. Crompton and A. I. McIntosh, Phys. Rev. Letters 18, 527 (1967); and private communication.

[8] R. J. W. Henry and N. F. Lane (to be published).

[9] A. G. Engelhardt and A. V. Phelps, Phys. Rev. 131, 2115 (1963).

[10] G. Bekefi and S. C. Brown, Phys. Rev. 112, 159 (1958).

PHYSICAL REVIEW VOLUME 184, NUMBER 1 5 AUGUST 1969

Pressure Effects of Foreign Gases on the Absorption Lines of Cesium. V. The Effects of Xenon and CF_4†

Shang Yi Ch'en, David E. Gilbert,* and Domingo K. L. Tan‡

Department of Physics, University of Oregon, Eugene, Oregon 97403

(Received 14 April 1969)

The shift, broadening, and asymmetry of the doublet components of the first member of the Cs principal series produced by various relative densities of Xe up to 47 are described. The shift of 17 other high-member doublets is also reported for Xe up to a relative density (rd) of 5. The effects due to Xe are very similar to those due to Kr. The shift, broadening, and asymmetry curves for Xe, although much more pronounced, have the same qualitative shape as our recently reported curves for Ar and Kr. The observed half-widths of various Cs lines produced by CF_4 are very similar to those produced by Xe, and the red shifts are close to those produced by Kr and Xe.

I. INTRODUCTION

This paper is the fifth in a series.[1] The experimental details and nomenclature are as reported in the earlier papers except that the spectrograph has been converted to a dual-beam instrument followed by an in-line electronic data processing system that enables the direct recording of the absorption coefficient as a function of wavelength. The Xe and CF_4 used was 99.995 and 99.7% pure, respectively. The relative densities (rd) of Xe were computed from the Beattie-Bridgeman equation.[2] Since the broadening and red shift produced by Xe is greater than that for the other rare gases (the separation of red satellites from the main line is also greater for Xe), these effects in the doublet components are more easily detected. CF_4 was chosen because it is a sizable, spherical molecule which would be expected to act like a heavy rare gas with mass and polarizability between those of Kr and Xe.

II. RESULTS

A. Shift of Various Cs Absorption Lines by Xenon

The red shift $\Delta\nu_m$ of the doublet components of the Cs resonance lines produced by Xe, hereafter abbreviated as Cs(1)/Xe, is shown in Fig. 1. A low-pressure region enlargement of Fig. 1 is given in curve A of Fig. 2, with scale A for shift. Curve B is for Cs(2)/Xe. An absence of an error flag indicates that the error for that point is smaller than the size of the mark. The difference in shift for the two doublet components was detected as shown, but is negligibly small for rd < 7.

The temperatures of the absorption tube and the corresponding Cs vapor pressures for this and for the other figures are given in the third and fourth columns of Table I.

It is quite evident that the plots for $\Delta\nu_m$ versus rd are not linear for the low-pressure range. This is also reported by Duperier[3] for his measurement of the shift of the $^2P_{3/2}$ component up to rd 12. Due to the nonlinearity of the curve, it is not really appropriate to give the slope of the curve. The values of the slopes for rd < 1 given in Table I are merely average values.

The general shape of Fig. 1 is similar to that for Cs(1)/Kr as previously reported.[4] Due to the increase in intensity and width of the red satellite when the rd of xenon is increased, the positions of the peaks of the two doublet lines were considerably influenced by the overlapping of the broadened satellites and lines. The separation[5]